heritage

MDPI

Article

An Experimental Study on the Effect of Water on Historic Brickwork Masonry

Domenico Giaccone [1,*], Ulderico Santamaria [1] and Marco Corradi [2]

[1] Department of Economics, Engineering, Society and Business Organization, University of Tuscia, 01100 Viterbo, Italy; santamaria@unitus.it

[2] Department of Engineering, University of Perugia, 06125 Perugia, Italy; marco.corradi@unipg.it

* Correspondence: d.giaccone@unitus.it; Tel.: +39-(0)761-357-645; Fax: +39-(0)761-357-676

Received: 13 December 2019; Accepted: 8 January 2020; Published: 10 January 2020

Abstract: Architectural heritage is deeply threatened by extreme weather events due to ongoing climatic change. Since these phenomena are becoming more and more serious, their effects cannot be neglected when a reliable assessment of a historic masonry structure is required. In this paper, the phenomenon of rising damp was studied, focusing on the influence of water on the unit weight of masonry walls made from fired clay bricks and lime mortar. This study consists of a basic experimental research on the variations in the unit weight of masonry undergoing an ageing treatment, which was simulated through some cycles of capillary water absorption and temperature changes. The experimental study proves that penetrating damp causes an increase in masonry unit weight of more than 20%. This basic result is significant in the structural assessment of historic masonry buildings. Subsequent papers will analyze the interaction with strengths parameters.

Keywords: water effect; historic masonry; architectural heritage; lime mortar; clay bricks

1. Introduction

Architectural heritage has always suffered damage, which is the result of the decay of the masonry materials that occurs over time. Restorers and other professional figures involved in its conservation can slow down this process, but natural hazards are more and more serious and their effects cannot be ignored.

Nowadays, the awareness that architectural heritage is deeply threatened by climate change is becoming ever more apparent [1–3]. Changes in average climatic conditions occurring over a long period of time, result in an increased frequency and intensity of extreme weather events, such as the rise in environmental temperature, relative humidity, and freeze-thaw cycles. These phenomena directly affect the physical, chemical, and biological mechanisms, which can cause the deterioration of construction materials and therefore of the cultural assets themselves. Measuring the effects of these phenomena is a necessary condition for the analysis of the heritage assets, and will allow us to undertake a reliable assessment of the risks facing such assets and decide on an appropriate course of action for their protection.

Water is one of the most serious causes of damage to masonry architectural heritage [4–6]. It is the main actor in hazards, which lead both to sudden and slow disasters, such as floods on the one hand, and precipitations and water intrusion on the other [7]. With an increased strain on resources for conservation and protection, these natural events represent a major threat to architectural heritage. Heavy rain falls and flooding recently struck many parts of Europe, causing heavy damages and the collapse of important heritage structures. The city walls of Amelia [8], Italy, Cockermouth Castle, UK [9,10], and the fortress of Magliano (Figure 1) [11], also in Italy, are examples of heritage masonry structures recently collapsed or damaged due to water-related issues.

(**a**)

(**b**)

Figure 1. Example of the effect of heavy and extended rainfalls: the city wall of the fortress of Magliano, Italy, suddenly collapsed in 2012: (**a**) before the collapse; (**b**) after.

If water penetrates from the ground, the rising damp phenomenon occurs. It can affect any building element which is close to the ground, such as the wall structures. Figure 2 shows two representative examples in Rome. The first relates to one of the *aulae* of the former Bath of Diocletian, now a National Museum, while the second relates to one of the lateral chapels of the *San Pietro in Vincoli* church.

(**a**)

Figure 2. *Cont.*

(**b**)

Figure 2. (**a**) Diocletian Bath, Rome; (**b**) *San Pietro in Vincoli* church, Rome, Italy.

The deterioration due to rising damp can be initiated by different factors linked to both the physical properties of the building's materials, such as porosity, and to errors in design, such as the lack of a water-proof system for the protection of the wall basement.

Rising damp triggers physical, chemical, and biological processes of alteration and deterioration, very often concurrently [12]. Visible signs (such as color change), environmental discomfort, and worsening of performances are some of the effects of these processes. The latter consists of several factors, including those concerning mechanical behavior. From this point of view, several authors have studied the problem, focusing mainly on the degradation in terms of ultimate strength and stiffness. In 1972, Stang et al. [13] carried out an extensive experimental campaign of tests on masonry walls made of fired clay bricks and lime mortar, and proved that water reduces the compressive strength of bricks, mortar, and masonry as a whole. Franzoni et al. [14] used masonry triplets made of fired clay bricks and cement mortar, and proved that water can cause a decrease in compressive and shear strength, as well as a non-relevant change in stiffness. Amde et al. [15] obtained similar results. They performed experiments on masonry specimens made of bricks and cement-lime mortar, and proved that the ratio between the compressive strength measured in wet and dry specimens is 0.81, while the ratio between the corresponding elastic moduli is 0.88. Graubohm and Brameshuber [16] studied the problem, also considering the effect of freeze-thaw cycles, concluding that the mechanical properties of the masonry are not significantly affected.

Knowing how these parameters change in a damaged building element compared to a healthy building, allows one to conduct a more reliable structural analysis; this is important to understand their behavior and prevent their ruin. Although these parameters are significant, they are not sufficient to define the mechanical behavior of the wall completely. In fact, in the simplest situations, one also needs to know, at the very least, the unit weight.

This study consists of a basic experimental research, which aims to investigate how the unit weight of masonry varies when it is affected by rising damp. This was done using a set of masonry specimens, which underwent an ageing treatment in the laboratory in order to simulate being exposed to severe environmental conditions.

Unit weight or weight density is defined as the ratio between the weight and the unit volume (usually, measured in kg/m^3). In the field of material science, two definitions of density are provided. Real density is the ratio between the weight of the solid particles and their volume. Apparent density is the ratio between the weight and the volume, also including internal voids.

Masonry can be considered a composite material with a heterogeneous and hierarchical structure, because it is an assemblage of units (such as bricks or stones) and mortar which, in turn, is a mixture of a binder and an aggregate. As a result of this structure, defining the density of the masonry is a difficult task, since it is influenced not only by the intrinsic physical properties of the constituent materials, but also by workmanship, method of construction, wall arrangement and deterioration. In a wall affected by rising damp, the voids are filled with water, which contributes to the increased weight of

the masonry itself. As a consequence, the apparent density and the weight density increase. Moreover, rising damp usually does not affect the whole wall, but only its lowest part. It is therefore appropriate to divide the wall into different homogeneous parts, and to assign to them the corresponding value of the weight density.

To simulate typical moisture conditions, Smith [17] proposed conjectural models, validated by data collected by other scholars [18–22]. From a macroscopic point of view, it is possible to recognize at least three sections in a wall affected by rising damp: the lowest, which is always characterized by a critical level of water content, the uppermost, where the amount of water is not to be considered pathological, and the intermediate, where the amount of water changes cyclically depending on the environmental conditions. The latter is delimited by the lowest and highest water marks, that is, two borderlines (MinBIh and MaxBIh), within which, the rising front ranges periodically. These borderlines identify iso-humidity (IH) surfaces, so called because each point of masonry belonging to them has the same content of water. Looking at the cross section of the wall, iso-humidity surfaces define, more or less, a Gaussian curve, as shown in Figure 3.

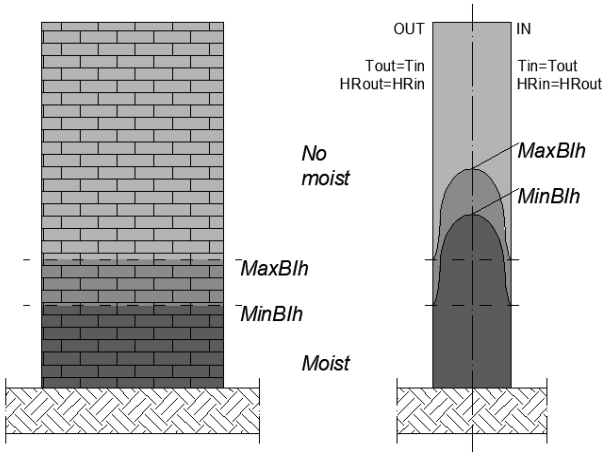

Figure 3. Typical situation of a masonry wall affected by rising damp.

Water, which rises from the ground and enters the masonry via capillary action, spreads in a way that is closely linked both to the brick bonding pattern and to the thermo-hygrometric conditions to which the two sides of the wall are exposed.

In a wall characterized by a homogeneous material and which has its sides exposed to the same environmental conditions, MinBIh and MaxBIh on both wall sides are approximately horizontal and have the same height from the ground. A schematic representation of this situation is shown in Figure 3.

In the past, several scholars proposed mathematical formulas to relate the height of the rising front to the other physical parameters that characterize the phenomenon [23–26]. The mechanism of moisture transport within a porous material is complex, thus, many parameters influence the height of the rising front. In actual conditions, a direct survey is the most reliable way to check the level of damage. It can be done by means of diagnostic instruments or through a sensitive experience, which is the simplest way. The lowest section of a wall affected by rising damp is easily recognizable thanks to the permanent change of color due to the wetting effect. In the intermediate section, the color changes cyclically, and efflorescences may be also found due to salts carried by the water being layered down before evaporating.

2. Materials and Methods

2.1. Preparing the Materials

This study was carried out on small brickwork masonry specimens, made of a few units joined by mortar courses (bed joints). They were made in the laboratory, following traditional building techniques and using materials readily available in northern Latium, Italy.

The units used for construction are fired clay bricks with nominal dimensions of 100 × 210 × 20 mm. They were manufactured in a local kiln following a traditional process consisting of several steps: hand-molding the pieces using wooden molds; natural drying; firing in a wood-fired oven reaching a temperature of about 1000 °C, for 85 h, consecutively; natural cooling for five days.

A pozzolanic mortar was used for construction. This was prepared by mixing three parts of aggregate and one of binder, according to a traditional method that already known by the Romans [27] and widely reproduced in the following centuries [28]. The mix was prepared in the laboratory where the environmental temperature was 24 °C and the relative humidity was 70%. Elements were mixed through a trowel, until an adequate blend and consistency was obtained. The water/binding ratio by volume was 1/4. The binder was a commercially available lime-putty, and its physical characteristics are summarized in Table 1. They were determined according to the EN 459-1 standard [29] and provided by the manufacturer. The aggregate consisted in a *pozzolana* came from a local quarry. It was characterized through a sieving test, performed in accordance with the EN 933-1 [30] standard. Test results are shown in Figure 4 and in Table 2.

The masonry specimens (Figure 5) reproduce a single-leaf wall with a stretching bonding pattern. According to bibliographical sources [31,32], experimental work aimed to characterize wet masonry is usually conducted on single-leaf masonry specimens with stacking or running bond patterns. In this study, the second was preferred because it allowed us to take into account vertical mortar joints (head joints). According to Massari [33], this is a significant feature because water rises with a different velocity in bricks and mortar joints due to their different responses to water intrusion.

Table 1. Properties of the lime putty.

Apparent Density	1300 kg/m^3
Type of lime	CL 90 S-PL
Grain size	min 98% lower than 0.1 mm
$CaCO_3$	max 4%

CL 90 S-PL = Calcium lime with CaO + MgO content ≥ 90%, in the form of lime putty, in accordance. with 4.4 of EN 459-1:2010.

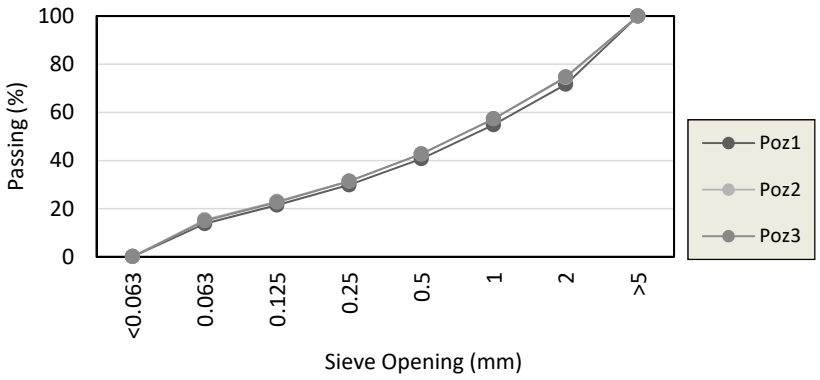

Figure 4. Grain-size distribution of the *pozzolana*.

Table 2. Cumulative passing fraction of *pozzolana* after the sieving test.

Sieve Size (mm)	Poz1	Poz2	Poz3
<0.063	0.09	0.09	0.03
0.063	13.77	14.95	15.37
0.125	21.46	22.66	22.97
0.25	29.84	31.37	31.42
0.5	40.72	42.74	42.69
1	54.86	57.28	57.36
2	71.65	74.71	74.41
>2	100	100	100

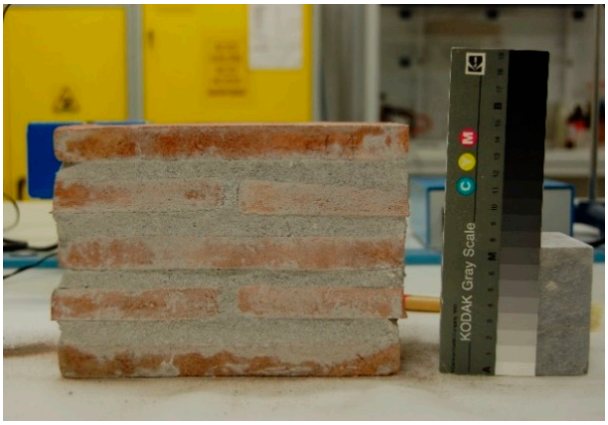

Figure 5. A brickwork masonry specimen.

Each masonry specimens had a nominal size of 100 × 210 × 155 mm. The ratio between the brick and the mortar volumes in each masonry specimen was 6:1. The ratio between the brick and bed joint thicknesses was 1.4. This value was rather low compared to that suggested by the "Rule of the Art" (i.e., technical expedients to respect the building and obtain the best structural performances), according to which the thickness of bed joints should be as small as possible. However, the use of thick bed joints was very common in Latium, especially during Roman times and the Middle Ages [34,35] (Figure 6).

Masonry specimens were constructed using the following process: several bricks were initially cut in half using a hand-held disc cutter with a diamond blade. Bricks were subsequently soaked in deionized water for a duration of about six hours, in order to prevent them from absorbing the water from the mortar joints. Meanwhile, the lime mortar was prepared and specimens were assembled. They were left outdoors for curing, for a duration of four months, sheltered from rain and wind, in thermo-hygrometric conditions that allowed for the phenomenon of setting without the risk of deterioration [Temperature (T) = 18–20 °C; Relative Humidity (HR) = 80%–95%].

In addition to masonry specimens, six brick specimens, measuring 20 × 20 × 20 mm, were cut out from one brick, and three mortar specimens, 40 × 40 × 40 mm in dimensions, were made by pouring the same mixture used for the construction of the masonry specimens into polymethylmethacrylate (PMMA) molds. The complete set of the specimens is shown in Figure 7. The specimens are designated by an alphanumeric code: two letters specified the type of material (Br = Brick, Mo = Mortar, Ma = Masonry) while a number was used to identify each tested specimen.

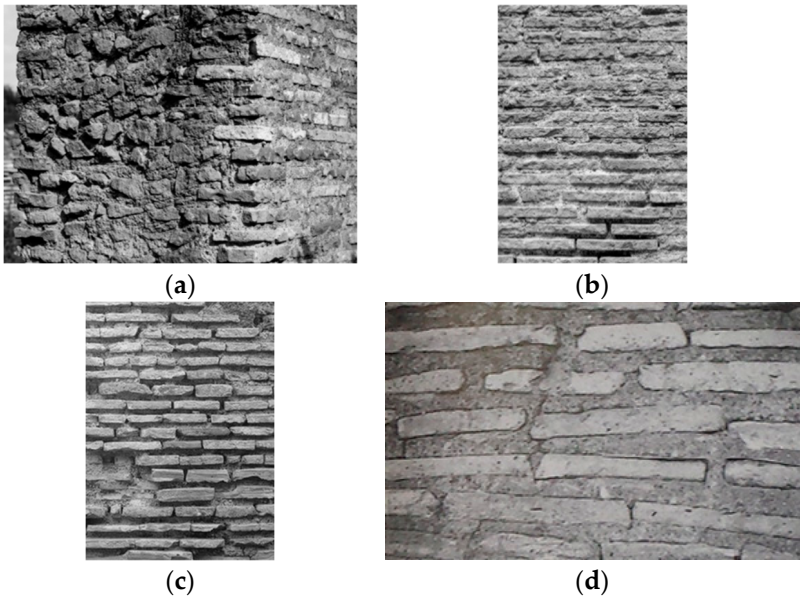

Figure 6. Examples of historic brickwork masonry with thick bed joints: (**a**) the archaeological site of Ostia Antica; (**b**) the Baths of Caracalla, Rome; (**c**) the Flavian Amphitheatre (*Colosseum*), Rome; (**d**) the *Santi Nereo e Achilleo* church, Rome, Italy.

Figure 7. Different typologies of tested specimens (letter designation: Br = Brick, Mo= Mortar, Ma = Masonry).

Tests were carried out in order to get information about their response to water. Several studies propose to use Fick's laws to study the diffusion of moisture in a porous material [36–38]. Fick's first law relates to the flux of the diffusing substance through the unit area of a section, to the concentration gradient, measured normal to the section, by means of the diffusion coefficient, in a steady state. Fick's second law is used to study the diffusion in a dynamic condition, i.e., to consider the time-dependence. The simplest form of the two Fick's laws is:

$$F = -D\frac{dC}{dx}, \tag{1}$$

$$\frac{dC}{dt} = D\frac{d^2C}{dx^2}, \tag{2}$$

where: F (m/s) is the diffusion flux per unit area of section; C (%) is the concentration of diffusing substance; x (m) is the space coordinate measured normal to the section; D (m^2/s) is the diffusion coefficient; t (s) is the time.

These laws can be used for thin and homogeneous specimens, and in this case the solutions to the equations can be easily obtained [39,40]. For 3D (three-dimensional) specimens (i.e., prisms), the equations and their solutions are more complex. Moreover, generally the diffusion coefficient D can depend on the concentration of the diffusing substance C, and on the homogeneity of the specimen. For this reason, it is usually determined experimentally [41–43].

The tests for the determination of the water absorption by capillarity, the water absorption at atmospheric pressure, and the drying properties were performed according to the standards EN 15801 [44], EN 13755 [45], and EN 16322 [46], respectively. The requirements of the EN 13755 standard were partially changed and adapted to the specific test program: deionized water was used instead of tap water in order to avoid the introduction of external salts into the tested materials. For the brick and masonry specimens, the ratio between the surface area and the apparent volume was 0.30 and 0.04 mm^{-1}, respectively. The geometrical features of the specimens are summarized in Table 3.

Table 3. Geometrical properties of the specimens.

Material	Number of Specimens	Dimensions (mm)	Volume (mm^3)	Total Surface Area (mm^2)	Base Surface Area (mm^2)	Total Surface Area/Volume (mm^{-1})
Brick	6	$20 \times 20 \times 20$	8.0×10^3	2.40×10^3	4.0×10^2	0.30
Mortar	3	$40 \times 40 \times 40$	6.4×10^4	9.60×10^3	1.6×10^3	0.15
Masonry	3	$100 \times 210 \times 155$	3.25×10^6	1.38×10^5	2.1×10^4	0.04

The specimens used for this study are prisms, and the masonry ones are also layered. According to the experiment design, the flux of the water occurs in all three directions. These conditions make Fick's laws difficult to apply. However, other tests were carried out in order to get information about the attitude of specimens toward water.

Data derived from these tests were used to calculate the water absorption coefficient by capillary action (AC), the water absorption coefficient at atmospheric pressure (Ab), the drying index (ID), and the flow velocity of the water (v) 24 h after the beginning of the tests. The latter was determined by using the following inverted formula of the mass flow rate:

$$v = \frac{m}{\rho \times A}, \tag{3}$$

where $\dot{m}$ is the mass flow rate (kg/s), ϱ is the weight density of water (0.997 g/ml at 24 °C), and A is the absorbent/dispersive surface (m^2), that is the base surface area (for absorption by capillarity) or the total surface area. In addition to these tests, the masonry specimens were weighted with a 1g-precision scale, and their surface temperature was measured with a Protimeter MMS2 BLD8800 digital thermo-hygrometer. Moreover, specimens were photographed, and their color was recorded both in the correspondence of the bricks and the mortar by making a comparison with the palettes, which are in the Munsell Book of Colors [47,48]. After this phase, the masonry specimens underwent an ageing treatment, specifically designed to simulate the effects of wetting/drying cycles, induced by rising damp and temperature changes.

2.2. The Ageing Treatment

The ageing treatment was drawn up starting from the past experimental processes described in [34,35] and from relevant standards [49–52]. The aim was to study the effect of placing the specimens in contact with water and exposing them to thermal variations. The ageing treatment (the duration of exposure to low and high temperatures, a number of cycles, and a range of temperatures) was chosen in such a way that the specimens underwent a thermal excursion comparable to those occurring in actual situations. Specimens were initially dried in an oven at 60 ± 5 °C for a duration of 48 h, photographed and weighed, and their surface temperature was measured. Then, they were placed into closed PMMA

boxes, laid on a 5 mm thick absorbent paper substrate soaked with distilled water. They remained in this condition for seven days, during which water was absorbed by capillary action (Figure 8).

Subsequently, each specimen was inserted into a polyethylene (PE) bag in order to protect it (Figure 9), and was buried in a refrigerating mixture made by adding 23 g of sodium chloride per kg of ice (Figure 10). Specimens were left curing for 8 h. During this period, the environmental temperature gradually reduced to −18 °C, and then increased again. As a consequence of this, the surface temperature of the specimens was also varied in order to reach the thermal equilibrium. Finally, the specimens were removed from the PE bags and placed into the oven at 60 °C for 16 h (Figure 11).

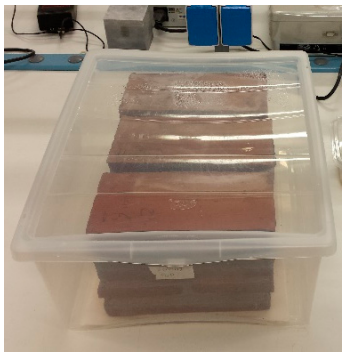

Figure 8. Masonry specimens inside the polymethylmethacrylate (PMMA) boxes.

Figure 9. Masonry specimens inside the polyethylene (PE) bags.

At the end of the ageing treatment, specimens were weighed and photographed again, and the surface temperature was recorded. They were re-placed into the PMMA boxes, over a sheet of soaked paper, and underwent a new ageing cycle. This was repeated 8 times. During this period, specimens were accurately weighed on a daily (24 h) basis in order to record the amount of absorbed water. At the end of the 8 cycles, a full photographic survey was undertaken, in order to analyze the level of damage [53]. The color change was also examined, both in the bricks and in the mortar.

Figure 10. Masonry specimens buried in the refrigerating mixture.

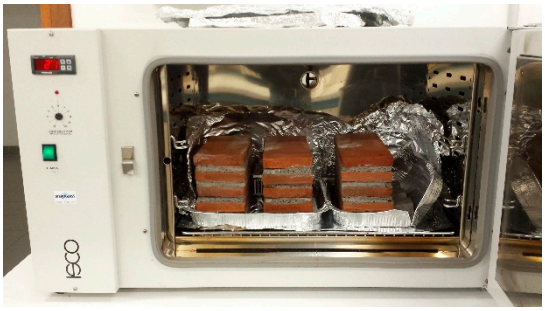

Figure 11. Masonry specimens in the oven.

3. Results and Discussion

3.1. Results

Treated masonry specimens showed a change of color, compared to the untreated ones. Test results related to the bricks and the mortar joints are summarized in Table 4 and Figure 12.

Table 4. Color changes of the bricks and mortar.

Condition		Hue	Value	Chroma	Reflectivity (%)
Un-	Brick	5YR	6	4	-
Treated	Brick	7.5YR	6	4	-
	Mortar	7.75N	7	0	54.80
	Mortar	7.5N	7	0	50.70
	Brick	5YR	4	4	-
Treated	Brick	7.5YR	4	4	-
	Mortar	10G	5	1	-
	Mortar	5G	5	1	-

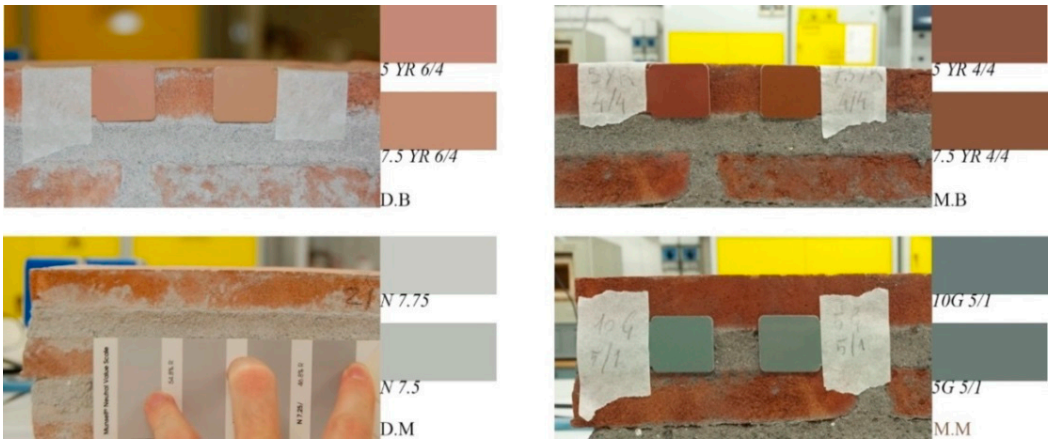

Figure 12. Color changes between the untreated (**left**) and the treated (**right**) bricks and mortar joints.

According to the Munsell reference [47,48], the color of any material can be defined using three components that are Hue, Value (degree of lightness/darkness), and Chroma (color purity). By referring the masonry specimens used in this research, the color of the bricks changed from a dull orange to a dull reddish brown, that is, Hue and Chroma did not change, while Value decreased. With regards to the mortar joints in an untreated condition, these were a greenish white, belonging to the neutral color palettes, while, after treatment, they turned to greenish grey, belonging to the green tonal palettes.

The response of the brick, mortar, and masonry specimens toward water intrusion and release was studied according to standard tests. AC, Ab, and ID were determined, and the flow velocity (v) of the water that was absorbed or released was also calculated using Equation (3).

With regards to absorption by capillary action, the test results are summarized in Table 5, while Figures 13–15 show the amount of water absorbed by the three different types of specimens as a function of the square root of the time. Bricks and mortar absorbed a high amount of the water in the first hour of the test, while the absorption rate was almost constant for masonry specimens. It can be noted that the flow velocity was higher in the mortar than in the brick and masonry specimens.

Table 5. Water absorption by capillary action (mean test conditions: T = 24 °C, relative humidity (HR) = 53%).

	AsA (mm^2)	W_{bAT} (g)	W_{Dry} (g)	W_{cap24h} (g)	M_{cap24h} (%)	W_{cap7d} (g)	M_{cap7d} (%)	v (m/s)	AC ($kg/m^2\ s^{0.5}$)
Brick	4×10^2	14.14	13.93	16.63	16.23	16.76	20.31	1.07×10^{-6}	0.07
(StD)		(0.11)	(0.09)	(0.08)		(0.11)			
Mortar	1.6×10^3	78.86	78.06	105.43	25.96	106.65	36.62	2.73×10^{-6}	0.23
(StD)		(0.82)	(0.91)	(0.95)		(0.85)			
Masonry	2.1×10^4	5012	4957	5294	6.79	5834	17.69	7.80×10^{-7}	0.09
(StD)		(39)	(37)	(35)		(68)			

AsA = absorbing surface area, W_{bAP} = weight of the specimens before the ageing treatment, W_{Dry} = weight of the specimens dried by oven, W_{cap24h} = weight of the specimens 24 h after the beginning of the test, M_{cap24h} = mass of water absorbed by the specimens 24 h after the beginning of the test, W_{cap7d} = weight of the specimens 7 days after the beginning of the test, M_{cap7d} = amount of water absorbed by capillarity 7 days after the beginning of the test, v = flow velocity, AC = capillary water absorption coefficient, and StD = standard deviation.

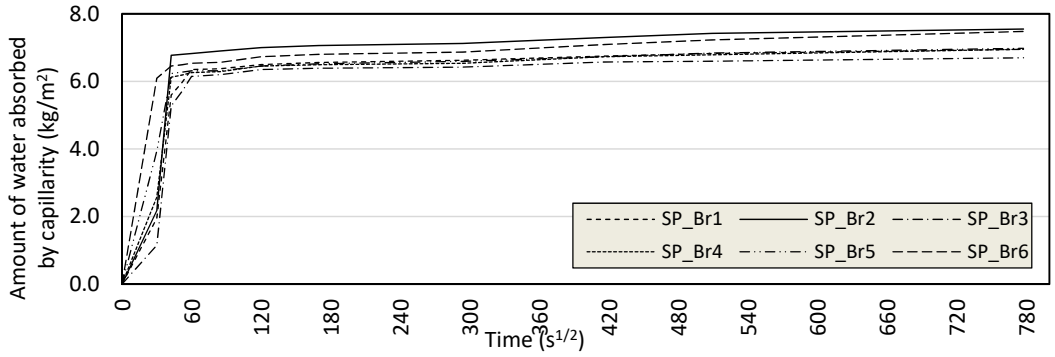

Figure 13. Water absorbed by capillary action (brick specimens).

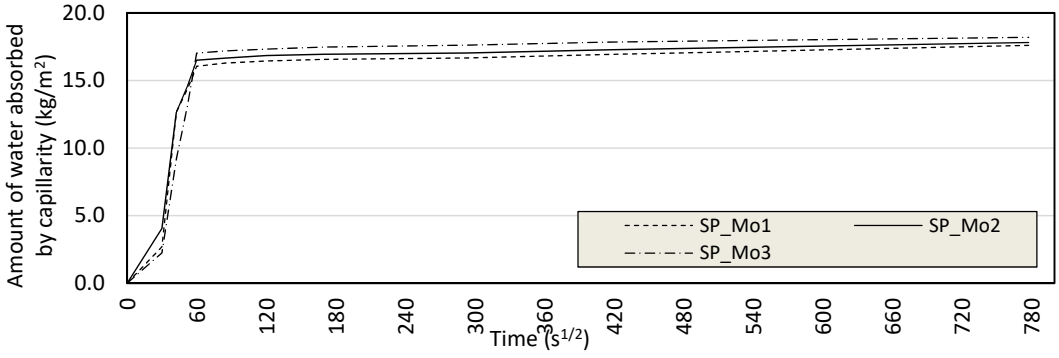

Figure 14. Water absorbed by capillary action (mortar specimens).

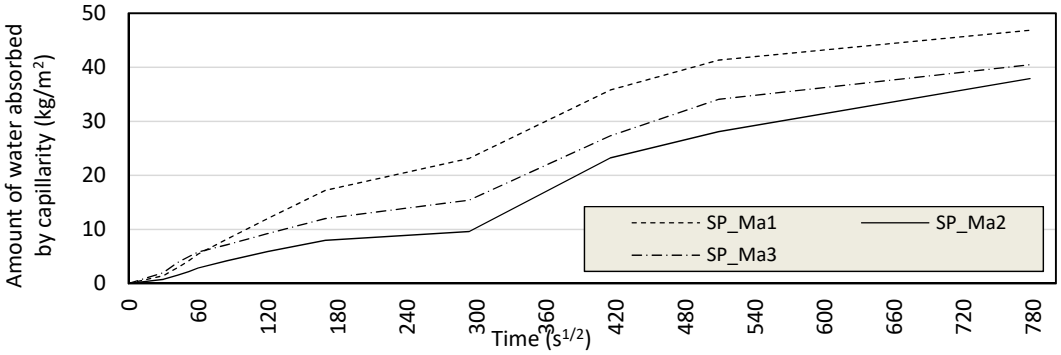

Figure 15. Water absorbed by capillary action (masonry specimens).

With regards to absorption at atmospheric pressure, the test results are summarized in Table 6. These results are consistent with the ones obtained from the previous tests, but the amount of water absorbed both after 24 h and 7 days is now smaller because of the larger dimensions of the absorbing surface area.

For the drying test, results are summarized in Table 7, and the drying curves related to the brick, mortar, and masonry specimens are shown in Figures 16–18, respectively. Since the specimens were initially fully imbibed, the maximum amount of water contained by the specimens at the beginning of the test was 20.45%, 39.52%, and 24.93% of the dry mass of the bricks, mortar, and masonry, respectively. For the bricks, it is possible to distinguish two drying phases (Figure 16): the water content highly decreased during the first 12 days of drying, while it stayed almost constant for the remaining 22 days. On the other hand, for the mortar and masonry specimens, the loss of water during the drying process had a constant negative gradient (Figures 17 and 18). The drying process was rather slow for all specimens. This is proved both by the timeframe and by the values of the flow velocity, which was several times lower compared to the absorption tests (Table 6). The weight of the bricks and mortar specimens stabilized (i.e., it decreased by 0.06% and 0.74%, respectively, between two measures in a row) after 34 and 36 days, respectively, while the masonry specimens did not reach this condition; in this experiment, the test was interrupted after 34 days. In order to compare these data with those referred to in the absorption tests, Table 7 reports the weight of the specimens after 7 days. The amount of water lost by the bricks during this period was less than half of that absorbed, while for the mortar and masonry specimens, it was less than a fifth and a tenth, respectively.

The test results demonstrate that the mortar, brick, and masonry exhibit a very different response toward absorbing and releasing water, in terms of both the amount absorbed/released and the velocity. Moreover, the tests reveal that the behavior of the masonry specimens cannot be defined as a sum of the behaviors of their construction materials. Test results also demonstrate the critical influence of the bonding pattern.

Table 6. Water absorption at atmospheric pressure (mean test conditions: T = 24 °C, HR = 53%).

	AsA (mm^2)	W_{bAP} (g)	W_{Dry} (g)	W_{Ab24h} (g)	M_{Ab24h} (%)	W_{Ab7d} (g)	M_{Ab7d} (%)	v (m/s)	Ab (%)
Brick	2.4×10^3	14.14	13.93	16.67	19.67	16.79	20.53	1.84×10^{-7}	20.53
(StD)		(0.11)	(0.09)	(0.13)		(0.13)			
Mortar	9.6×10^3	78.86	78.06	106.0	35.84	108.9	39.52	4.82×10^{-7}	38.09
(StD)		(0.82)	(0.91)	(0.87)		(0.86)			
Masonry	1.38×10^5	5012	4957	5382	8.57	6202	25.11	1.49×10^{-7}	25.11
(StD)		(39)	(37)	(51)		(75)			

W_{Ab24h} = weight of the specimens 24 h after the beginning of the test, M_{Ab24h} = mass of the water absorbed by the specimens 24 h after the beginning of the test, W_{Ab7d} = weight of the specimens after 7 days, M_{Ab7d} = mass of the water absorbed by the specimens after 7 days, Ab = water absorption coefficient at atmospheric pressure.

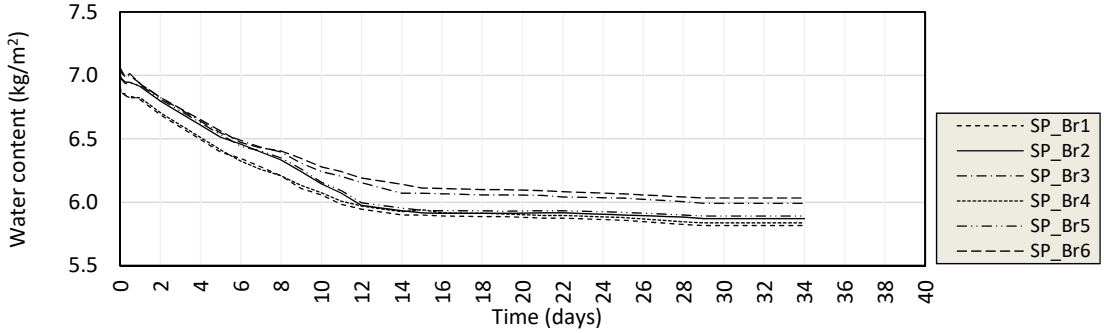

Figure 16. Drying test. Amount of water vs. time (brick specimens).

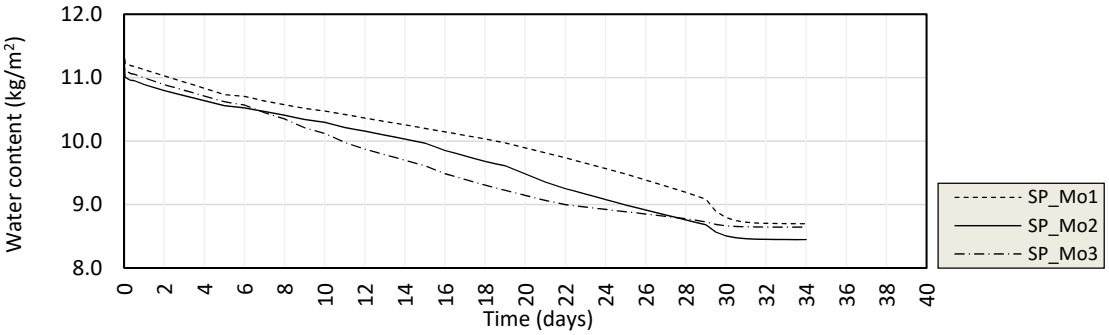

Figure 17. Drying test. Amount of water vs. time (mortar specimens).

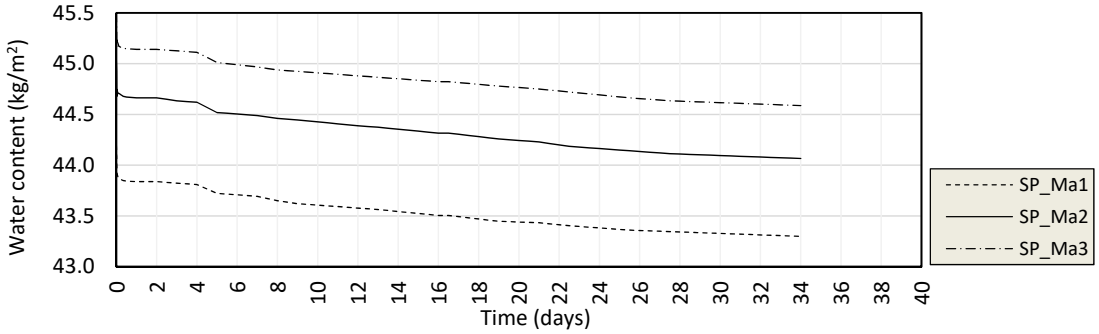

Figure 18. Drying test. Amount of water vs. time (masonry specimens).

Table 7. Water release by natural drying (mean test conditions: T = 24 °C HR = 53%).

	DsA (mm^2)	W_{bAP} (g)	W_{Ab7d} (g)	W_{Dry24h} (g)	M_{Dry24h} (%)	W_{Dry7d} (g)	M_{Dry7d} (%)	v (m/s)	ID (-)
Brick	2.4×10^3	14.14	13.93	16.54	−1.51	15.28	−9.13	-1.79×10^{-8}	0.87
(StD)		(0.11)	(0.09)	(0.13)		(0.17)			
Mortar	9.6×10^3	78.86	78.06	105.6	−2.99	100.9	−7.30	-5.62×10^{-8}	0.85
(StD)		(0.82)	(0.91)	(0.92)		(0.80)			
Masonry	1.38×10^5	5012	4957	6152	−0.80	6129	−1.18	-1.91×10^{-8}	0.98
(StD)		(39)	(37)	(74)		(72)			

DsA = dispersant surface area, W_{Ab7d} = weight of the specimens before drying, W_{Dry24h} = weight of the specimens after 24 h of natural drying, M_{Dry24h} = mass of the water lost by natural drying after 24 h, W_{Dry7d} = weight of the specimens after 7 days of natural drying, M_{Dry7d} = mass of the water lost by natural drying after 7 days, ID = Drying Index.

3.2. The Ageing Treatment

Curves in Figure 19 show the gain of weight of the three masonry specimens during the ageing treatment. Figure 20 shows the amount of water absorbed by masonry specimens during each ageing cycle. Figure 21 shows the maximum and minimum values of the weight measured for each cycle.

They are averaged over the three specimens and related to the respective mean values over the last seven cycles (dashed line and continuous line), and to the mean value before the start of the ageing treatment (dashed-dot line).

The weight of the masonry specimens increased by 16.40% (from 5012 g to 5834 g) during the first ageing cycle, and it further increased by 5.71% during the second (from 5834 g to 6167 g). The minimum and maximum values of the weight stabilized at the end of the second and third cycles, respectively. The mean values were 6008 g and 6165 g, respectively, corresponding to an increase of 19.87% and 23.01% from the initial weight (5012 g). The standard deviation was 14.51 and 18.75 g in the second. These two values were the thresholds within which the weight of the treated masonry specimens varied. The latter is very similar to that obtained from the absorption test at atmospheric pressure (6202 g).

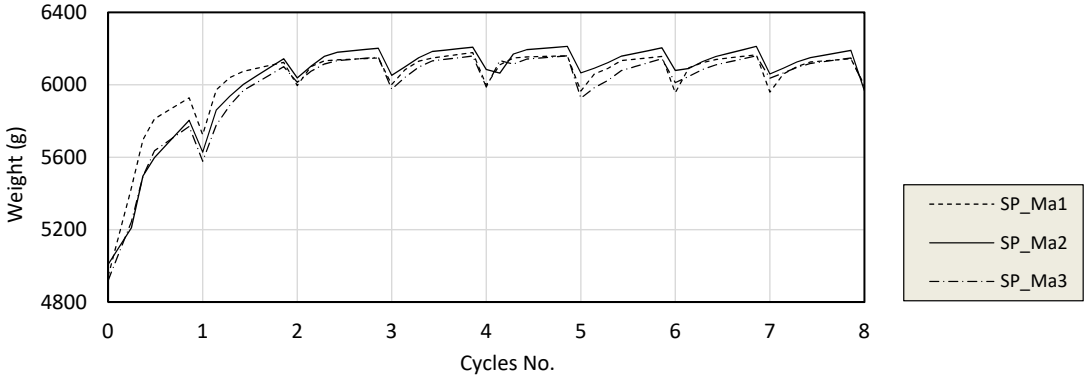

Figure 19. Weight per cycle (masonry specimens).

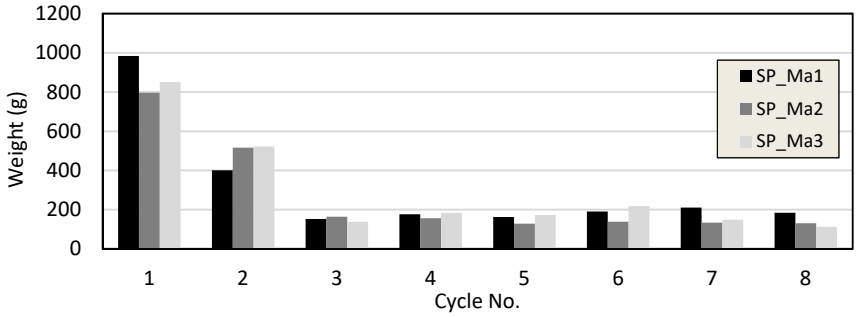

Figure 20. Weight of absorbed water (masonry specimens).

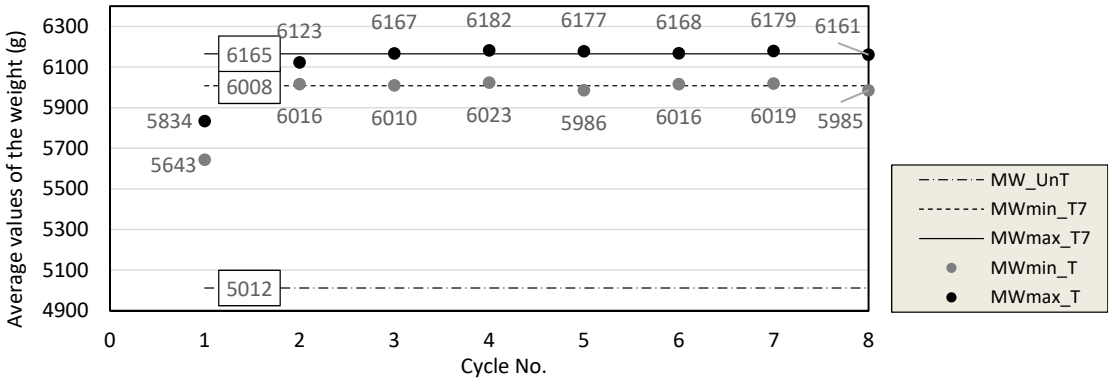

Figure 21. Average values of the weight over each cycle (masonry specimens). MW_UnT = mean weight of the untreated specimens, MWmin_T = minimum mean weight of the treated specimens, MWmax_T = maximum mean weight of the treated specimens, MWmin_T7 = minimum mean weight of the treated specimens over the last seven cycles, MWmax_T7 = maximum mean weight of the treated specimens over the last seven cycles.

Table 8 shows the weight values of the untreated and treated masonry specimens. For the treated specimens, seven weight values are reported: one for each step (i.e., 24-h treatment) of the ageing treatment. The values were calculated as the arithmetic mean among the three specimens, and were averaged across the last seven cycles. Starting from these data, the unit weight of the untreated and treated specimens was determined.

Table 9 reports the values of the environmental parameters, i.e., temperature (T_{env}) and HR, the surface temperature (T_{surf}), and the mean values of the weights (W). It is worth noting that the specimens were exposed to a severe temperature (ranging between +60 and −18 °C). However, during each cycle, their surface temperature ranged from −5.2 to +46.1 °C. These values reflect the actual weather conditions in the Italian Mediterranean regions [54]. The severe thermal excursions simulate an extreme weather event, which is one of the most significant effects of the ongoing climate change [55].

Table 8. Mean values of the weights (masonry specimens) over one cycle.

		Un-Treated Specimens	Treated Specimens						
			Step 1	Step 2	Step 3	Step 4	Step 5	Step 6	Step 7
MW	(g)	5012	6007	6101	6132	6148	6154	6159	6165
(StD)		(39)	(74)	(60)	(47)	(37)	(28)	(19)	(14)
ΔW1	(%)	0.00	19.9	21.7	22.4	22.7	22.8	22.9	23.0
ΔW2	(%)	-	0.00	1.56	2.07	2.34	2.44	2.53	2.62
W	(kg/m^3)	1540	1845	1874	1884	1889	1891	1892	1894

MW = mean weight, ΔW1 = weight increment (%) compared to the weight of untreated specimens, ΔW2 = weight increment (%) compared to the weight at Step 1.

Table 9. Mean values of the HR, T_{env}, T_{surf}, and the weight of masonry specimens in different conditions.

Conditions	HR (%)	T_{env} (°C)	T_{surf} (°C)	W (g)
Untreated	40	20.8	20.4	5012
Before ice	34	21.5	21.3	6165
In ice (−18 °C)	100	−18.0	−5.2	-
After oven (+60 °C)	37	20.6	46.1	6008

4. Conclusions

In this paper, the results of an experimental study on the effect of water on the unit weight of brickwork masonry have been presented. Experimental tests were carried out on masonry specimens made of fired clay bricks and lime mortar that were exposed to an ageing treatment. During each wetting/drying cycle, the amount of water, absorbed and rejected by masonry specimens, varied over time, causing a change in their weight.

The recorded data allowed us to quantify the increase in the unit weight of the masonry due a water-based treatment. This increase consisted of two rates. The first one is constant, permanent, and is about 19% of the unit weight of the masonry with a no-pathological water content. The second-rate ranged between 19% and 23% depending on the environmental conditions inducted during the ageing treatment. The increase in masonry unit weight was rather fast, and it concentrated in the first two ageing cycles.

The ageing treatment reproduced through the experiment was chosen considering the typical conditions of historic masonry structures affected by rising damp. Since the test results demonstrate that the increase in the unit weight was not negligible, its effect should be considered to assess the structural response of masonry buildings. For this reason, it is important to identify the areas of a building affected by damp.

Tests carried out on brick, mortar, and masonry specimens highlighted their different behavior toward water intrusion and rejection. This means that data obtained through the conducted experiment are specific and linked to the type of brickwork masonry. This could be considered a limitation of

this research. However, some interesting conclusions can be drawn. Test results reveal that mortar joints absorb and reject more water than brick, and that they do so more rapidly. For this reason, it is expected that the brick's height/bed joint ratio is a meaningful parameter to estimate the increase of the masonry unit weight during ageing. In this experiment, the brick's height/bed joint ratio was 1.4. More tests will be necessary to confirm this, but the emerging trend seems sufficiently clear. Moreover, it could also be interesting to consider other types of construction materials and extend the study to other types of masonry, such as stone masonry, or multi-leaf masonry.

The results of this experiment could be used in conjunction with previous research evidence to demonstrate that the pathological presence of water in brickwork masonry can lead to a significant decline in its mechanical properties. When acting forces are inertial (i.e., earthquake loading), an increase in a masonry's unit weight may further worsen the structural response of a historic masonry building.

Author Contributions: Conceptualization, U.S.; methodology, D.G. and M.C.; formal analysis, D.G.; writing—original draft preparation, D.G.; writing—review and editing, M.C. and D.G. All authors have read and agreed to the published version of the manuscript.

Funding: This work has been supported by the STORM E.C. project H2020-DRS-11-2015. 700191.

Acknowledgments: The authors would like to acknowledge the assistance of Alessio Molinari (Structures Laboratory, University of Perugia. Italy).

Conflicts of Interest: The authors declare no conflict of interest.

References

1. Booth, C.A.; Hammond, F.N.; Proverbs, D.G.; Lamond, J. *Solutions for Climate Change Challenges in the Built Environment*; John Wiley & Sons: Hoboken, NJ, USA, 2012; Volume 5.
2. D'Ayala, D.; Aktas, Y.D. Moisture dynamics in the masonry fabric of historic buildings subjected to wind-driven rain and flooding. *Build. Environ.* **2016**, *104*, 208–220. [CrossRef]
3. Cavalagli, N.; Kita, A.; Castaldo, V.L.; Pisello, A.L.; Ubertini, F. Hierarchical environmental risk mapping of material degradation in historic masonry buildings: An integrated approach considering climate change and structural damage. *Constr. Build. Mater.* **2019**, *215*, 998–1014. [CrossRef]
4. Franzoni, E. State-of-the-art on methods for reducing rising damp in masonry. *J. Cult. Herit.* **2018**, *31*, S3–S9. [CrossRef]
5. Borri, A.; Corradi, M. Architectural heritage: A discussion on conservation and safety. *Heritage* **2019**, *2*, 631–647. [CrossRef]
6. Wang, J.J. Flood risk maps to cultural heritage: Measures and process. *J. Cult. Herit.* **2015**, *16*, 210–220. [CrossRef]
7. STORM Project, Document Ref. D6.1 Classification of Hazards and Climate Change-related Events. Available online: http://www.storm-project.eu/wp-content/uploads/2017/04/D6.1-STORM-Models-for-the-Content-Management.pdf (accessed on 28 November 2019).
8. Ercoli, M.; Brigante, R.; Radicioni, F.; Pauselli, C.; Mazzocca, M.; Centi, G.; Stoppini, A. Inside the polygonal walls of Amelia (Central Italy): A multidisciplinary data integration, encompassing geodetic monitoring and geophysical prospections. *J. Appl. Geophys.* **2016**, *127*, 31–44. [CrossRef]
9. Creighton, O.H. *Castles and Castle Building in Town and Country*; Maney Publishing: Leeds, UK, 2005.
10. Spencer, P.; Faulkner, D.; Perkins, I.; Lindsay, D.; Dixon, G.; Parkes, M.; Parkes, A. The floods of December 2015 in northern England: Description of the events and possible implications for flood hydrology in the UK. *Hydrol. Res.* **2017**, *49*, 568–596. [CrossRef]
11. Andreini, M.; De Falco, A.; Giresini, L.; Sassu, M. Recenti eventi di crollo in mura storiche urbane. In Proceedings of the 3rd Conference Ingegneria Forense- su CRolli, Affidabilità Strutturale, Consolidamento (IF CRASC'15), Rome, Italy, 14–16 May 2015; Flaccovio: Palermo, Italy, 2015; pp. 239–250. (In Italian)
12. Amoroso, G. *Trattato di Scienza della Conservazione dei Monumenti. Etica della Conservazione, Degrado dei Monumenti, Interventi Conservativi, Consolidanti e Protettivi*; Alinea: Florence, Italy, 2002; pp. 91–130. (In Italian)
13. Stang, A.H.; Parsons, D.E.; McBurney, J.W. Compressive strength of clay brick walls. *Bur. Stand. J. Res.* **1929**, *3*, 507–571. [CrossRef]

14. Franzoni, E.; Gentilini, C.; Graziani, G.; Bandini, S. Mechanical properties of fired-clay brick masonry models in moist and dry conditions. *Key Eng. Mater.* **2014**, *624*, 307–312.
15. Amde, A.M.; Martin, J.V.; Colville, J. The effects of moisture on compressive strength and modulus of brick masonry. In Proceedings of the 13th International Brick and Block Masonry Conference, Amsterdam, The Netherlands, 4–7 July 2004.
16. Graubohm, M.; Brameshuber, W. Rehabilitation of Masonry constructions temporarily submerged by Water-influence of Water on the properties of Masonry and Facings, Drying Methods and their Effect. In Proceedings of the 11th Canadian Masonry Symposium, Toronto, ON, Canada, 31 May–3 June 2009.
17. Smith, B.M. *Moisture Problems in Historic Masonry Walls: Diagnosis and Treatment*; U.S. Government Printing Office: Washington, DC, USA, 1984.
18. Falchi, L.; Slanzi, D.; Balliana, E.; Driussi, G.; Zendri, E. Rising damp in historical buildings: A Venetian perspective. *Build. Environ.* **2018**, *131*, 117–127. [CrossRef]
19. Hola, A. Measuring of the moisture content in brick walls of historical buildings–the overview of methods. *IOP Conf. Ser. Mater. Sci. Eng.* **2017**, *251*, 012067. [CrossRef]
20. Hoła, A.; Matkowski, Z.; Hoła, J. Analysis of the moisture content of masonry walls in historical buildings using the basement of a medieval town hall as an example. *Procedia Eng.* **2017**, *172*, 363–368. [CrossRef]
21. Hoła, J.; Matkowski, Z.; Schabowicz, K.; Sikora, J.; Nita, K.; Wójtowicz, S. Identification of moisture content in brick walls by means of impedance tomography. *COMPEL Int. J. Comput. Math. Electr. Electron. Eng.* **2012**, *31*, 1774–1792. [CrossRef]
22. Sass, O.; Viles, H.A. How wet are these walls? Testing a novel technique for measuring moisture in ruined walls. *J. Cult. Herit.* **2006**, *7*, 257–263. [CrossRef]
23. Jurin, J. An account of some experiments shown before the Royal Society; with an enquiry into the cause of some of the ascent and suspension of water in capillary tubes. *Philos. Trans. R. Soc. Lond.* **1718**, *355*, 739–747.
24. Jurin, J. An account of some new experiments, relating to the action of glass tubes upon water and quicksilver. *Philos. Trans. R. Soc. Lond.* **1719**, *363*, 1083–1096.
25. Mason, G. Rising damp. *Build. Sci.* **1974**, *9*, 227–231. [CrossRef]
26. Hall, C.; Hoff, W.D. Rising damp: Capillary rise dynamics in walls. *Proc. R. Soc. A Math. Phys. Eng. Sci.* **2007**, *463*, 1871–1884. [CrossRef]
27. Adam, J.P. *Roman Buildings. Materials and Techniques*; Routledge: London, UK, 2005; pp. 129–134.
28. Arcolao, C. *Le Ricette del Restauro. Malte, Intonaci e Stucchi dal XV al XIX Secolo*; Marsilio: Venice, Italy, 1998. (In Italian)
29. EN 459-1. Building Lime. Part 1: Definitions, Specifications and Conformity Criteria. 2015. Available online: https://infostore.saiglobal.com/preview/98705147332.pdf?sku=877967_SAIG_NSAI_NSAI_2086537 (accessed on 28 November 2019).
30. EN 933-1. Tests for Geometrical Properties of Aggregates. Part 1: Determination of Particle Size Distribution. Sieving Method. 2012. Available online: https://www.scribd.com/doc/223990752/En-933-1-Tests-for-geometrical-properties-of-aggregates (accessed on 28 November 2019).
31. Sathiparan, N.; Rumeshkumar, U. Effect of moisture condition on mechanical behavior of low strength brick masonry. *J. Build. Eng.* **2018**, *17*, 23–31. [CrossRef]
32. Forghani, R.; Totoev, Y.; Kanjanabootra, S.; Davison, A. Experimental investigation of water penetration through semi-interlocking masonry walls. *J. Archit. Eng.* **2016**, *23*, 04016017. [CrossRef]
33. Massari, G.; Massari, I. Damp Buildings, Old and New. *Bull. Assoc. Preserv. Technol.* **1985**, *17*, 2–30. [CrossRef]
34. Marta, R. *Tecniche Costruttive a Roma nel Medioevo*; Kappa: Rome, Italy, 1989. (In Italian)
35. Montelli, E. *Tecniche Costruttive Murarie Medievali. Mattoni e Laterizi in Roma e nel Lazio fra X e XV Secolo*; L'Erma di Bretschneider: Rome, Italy, 2011. (In Italian)
36. Vu, H.T.; Tsotsas, E. Mass and heat transport models for analysis of the drying process in porous media: A review and numerical implementation. *Int. J. Chem. Eng.* **2018**, *2018*, 9456418. [CrossRef]
37. Ferretti, D.; Bazand, Z.P. Stability of ancient masonry towers: Moisture diffusion, carbonation and size effect. *Cem. Concr. Res.* **2006**, *36*, 1379–1388. [CrossRef]
38. De Freitas, V.P.; Abrantes, V.; Crausse, P. Moisture migration in building walls—Analysis of the interface phenomena. *Build. Environ.* **1996**, *31*, 99–108. [CrossRef]
39. Crank, J. *The Mathematics of Diffusion*, 2nd ed.; Oxford Science Publications: Oxford, UK, 1975.
40. Jaeger, J.C.; Carslaw, H.S. *Conduction of Heat in Solids*, 2nd ed.; Clarendon: Oxford, UK, 1959; pp. 176–187.

41. Zhang, J.; Hou, D.; Gao, Y.; Wei, S. Determination of moisture diffusion coefficient of concrete at early age from interior humidity measurements. *Dry. Technol.* **2011**, *29*, 689–696. [CrossRef]
42. Kassem, E.; Masad, E.; Lytton, R.; Bulut, R. Measurements of the moisture diffusion coefficient of asphalt mixtures and its relationship to mixture composition. *Int. J. Pavement Eng.* **2009**, *10*, 389–399. [CrossRef]
43. Post, N.L.; Riebel, F.; Zhou, A.; Keller, T.; Case, S.W.; Lesko, J.J. Investigation of 3D moisture diffusion coefficients and damage in a pultruded E-glass/polyester structural composite. *J. Compos. Mater.* **2009**, *43*, 75–96. [CrossRef]
44. EN 15801. Conservation of Cultural Property—Test Methods—Determination of Water Absorption by Capillarity. 2010. Available online: https://infostore.saiglobal.com/preview/98698597394.pdf?sku=873949_SAIG_NSAI_NSAI_2077869 (accessed on 28 November 2019).
45. EN 13755. Natural Stone Test Methods—Determination of Water Absorption at Atmospheric Pressure. 2008. Available online: https://infostore.saiglobal.com/en-us/standards/uni-en-13755-2008-1072611_SAIG_UNI_UNI_2499726/ (accessed on 28 November 2019).
46. EN 16322. Conservation of Cultural Heritage—Test Methods—Determination of Drying Properties. 2013. Available online: https://www.ds.dk/~{}/media/DS/Files/Downloads/udvalg/S-388/Udgivne-EN-standarder-CEN-TC-346---emneopdelt.ashx?la=da (accessed on 28 November 2019).
47. Glenn, J.J.; Killian, J.T. Trichromatic analysis of the Munsell Book of Color. *J. Opt. Soc. Am.* **1940**, *30*, 609–616. [CrossRef]
48. Newhall, S.M.; Nickerson, D.; Judd, D.B. Final report of the OSA subcommittee on the spacing of the Munsell colors. *J. Opt. Soc. Am.* **1943**, *33*, 385–418. [CrossRef]
49. Cultrone, G.; Sebastian, E.; Huertas, M.O. Durability of masonry systems: A laboratory study. *Constr. Build. Mater.* **2007**, *21*, 40–51. [CrossRef]
50. Uranjek, M.; Bosiljkov, B.V. Influence of freeze–thaw cycles on mechanical properties of historical brick masonry. *Constr. Build. Mater.* **2015**, *84*, 416–428. [CrossRef]
51. EN 11186. Cultural Heritage—Natural and Artificial Stones—Methodology for Exposure to Freeze—Thawing Cycles. 2008. Available online: https://www.ds.dk/~{}/media/DS/Files/Downloads/udvalg/S-388/Udgivne-EN-standarder-CEN-TC-346---emneopdelt.ashx?la=da (accessed on 28 November 2019).
52. Italian Code, No. 2233. Norme per L'accettazione dei Materiali Laterizi. 1939. (In Italian)
53. ICOMOS-ISCS. Illustrated Glossary on Stone Deterioration Patterns. 2008. Available online: https://www.icomos.org/publications/monuments_and_sites/15/pdf/Monuments_and_Sites_15_ISCS_Glossary_Stone.pdf (accessed on 29 November 2019).
54. Desiato, F.; Fioravanti, G.; Fraschetti, P.; Perconti, W.; Piervitali, E.; Pavan, V. Gli indicatori del clima in Italia nel 2018. *ISPRA Rep.* **2018**, *14*, 88. Available online: http://www.isprambiente.gov.it/files2019/pubblicazioni/stato-ambiente/SA_88_19_Indicatori_clima_annoXIV_2018.pdf (accessed on 29 November 2019). (In Italian).
55. Stoker, T.F.; Qin, D. *Climate Change 2013: The Physical Science Basis: Working Group I Contribution to the Fifth Assessment Report of the Intergovernmental Panel on Climate Change*; Stoker, T.F., Qin, D., Eds.; Cambridge University Press: Cambridge, UK, 2014. Available online: https://www.ipcc.ch/report/ar5/wg1/ (accessed on 29 November 2019).